European Journal of Neuroscience, Vol. 26, pp. 101–112, 2007 doi:10.1111/j.1460-9568.2007.05641.x

Environment enrichment rescues the neurodegenerative phenotypes in presenilins-deficient mice

Suzhen Dong, Chunxia Li, Pu Wu, Joe Z. Tsien and Yinghe Hu
Key Laboratory of Brain Functional Genomics, MOE&STCSM, Shanghai Institute of Brain Functional Genomics, East China Normal University, Shanghai, 3663 Zhongshan Road N., China 200062

Keywords: forebrain degeneration, immunity, inflammation, memory performance, neurodegeneration

Abstract

Presenilin (PS) 1 and 2 conditional double knockout (cDKO) mice show progressive memory dysfunction and forebrain degeneration. Gene expression profiling results revealed a strong activation of immunity and inflammation responses in the brains of 10-month-old cDKO mice. As environmental enrichment (EE) has been shown to be able to improve memory and induce neurogenesis of the brain, we assessed the effects of EE on the memory performance and the neurodegeneration in cDKO mice. We found that EE effectively enhanced memory and partially rescued the forebrain atrophy of the cDKO mice. Our results suggest that immunity and inflammation could play important roles in the neurodegeneration of cDKO mice. Furthermore, the beneficial effects of EE may be associated with the inhibition of the expression of immunity and inflammation-related genes in the brain.

Introduction

Alzheimer's disease (AD) is an age-related neurodegenerative disease that represents the most common cause of dementia among people aged 65 or older. Mutations in the presenilin (PS) genes have been shown to be associated with the early onset of AD (Haass, 1997; Price & Sisodia, 1998). Presenilin 1 (PS1) is an essential component of a multiprotein protease complex, termed γ-secretase, which is responsible for the intramembranous cleavage of the amyloid precursor protein to produce β amyloid (Aβ; De Strooper *et al*., 1998). Genetic linkage analysis of AD patients demonstrated that a second presenilin gene, presenilin 2 (PS2), was also involved in the early onset of AD (Levy-Lahad *et al*., 1995). Several knockout animal models have been generated to study the physiological function of PS genes. PS1 knockout mice were embryonic lethal, while forebrain-specific PS1 knockout mice were almost normal except that they lacked the enrichment-induced neurogenesis (Feng *et al*., 2001). However, PS2 knockout mice were viable, fertile, and exhibited no obvious abnormal phenotypes (Donoviel *et al*., 1999). Interestingly, mice lacking both PS1 and PS2 in the forebrain showed AD-like progressive neurodegenerative phenotypes (Beglopoulos *et al*., 2004; Saura *et al*., 2004). Only mild memory impairment was observed in the 2-month-old conditional double knock out (cDKO) mice, while severe memory dysfunction had started in the 6-month-old mice in Morris water maze task. In addition, the 2–6-month-old cDKO mice showed a progression of deficits in hippocampal synaptic plasticity. Furthermore, age-dependent brain atrophy was observed in the cDKO mice (Saura *et al*., 2004).

The classical paradigm of environmental enrichment (EE) involves placing animals in large cages that contain running wheels, colourful tunnels, and assorted toys. There is much evidence to indicate that EE could enhance the memory of normal (Nilsson *et al*., 1999; de Jong *et al*., 2000; Woodcock & Richardson, 2000; Duffy *et al*., 2001; Williams *et al*., 2001) as well as memory-deficient animals (Winocur, 1998; Lessard *et al*., 1999; Frick & Fernandez, 2003; Need *et al*., 2003). EE could also rescue the age-dependent memory decline in AD models (Arendash *et al*., 2004; Jankowsky *et al*., 2005). It has been reported that EE led to brain structural changes, including the elevation of brain weight, size (Rosenzweig & Bennett, 1969) and cortical thickness (Diamond *et al*., 1966) in different animal models. Animals exposed to EE exhibited the induction of dendritic spines, extent of neuronal branching (Kolb & Gibb, 1991; Rampon *et al*., 2000), elevation of numbers of synapses per neuron (Klintsova & Greenough, 1999), and induction of neurogenesis in the dentate gyrus (Kempermann *et al*., 1997). Furthermore, EE could delay onset and progression of several neurodegenerative diseases, such as AD (Jankowsky *et al*., 2005; Lazarov *et al*., 2005), Parkinson's disease (Faherty *et al*., 2005; Zhu *et al*., 2005) and Huntington's disease (van Dellen *et al*., 2000; Hockly *et al*., 2002) in different animal models. In this report, we exposed 1-month-old cDKO mice to EE for three hours everyday for a total of five months and examined the effects of EE on the neurodegenerative phenotypes in cDKO mice.

Materials and methods

Animals

cDKO mice on B6CBA background were generated as described previously (Donoviel *et al*., 1999; Feng *et al*., 2001; Saura *et al*., 2004; Feng *et al*., 2004). Age- and gender-matched mice with the same genetic background (B6CBA) served as wild-type (wt) control. All animal experiments were carried out in accordance with regulations for the administration of affairs concerning experimental animals by Chinese Ministry of Science & Technology (2004).

Environmental enrichment (EE)

One-month-old cDKO mice were randomly divided into two experimental groups. One group was kept in standard cages (naive group) and

Correspondence: Dr Yinghe Hu, as above.
E-mail: yhu@brain.ecnu.edu.cn

Received 8 January 2007, revised 13 May 2007, accepted 21 May 2007

the other group was allowed to explore an enriched environment for 3 h/day for 5 months (enriched group). EE was set as described previously (Rampon *et al.*, 2000). Food and water were available in the boxes. After 5-months EE treatment, both male and female mice were used in the behavioural tests. There is no significant difference between male and female mice ($P > 0.1$) in all behavioural performances.

Behavioural tests

Open field test and novel object recognition task

Open field activity was measured in a 15 × 15-cm black box. Five minutes free locomotion was tracked by Digbev Open Field software. The novel object recognition experiment was performed as described previously (Feng *et al.*, 2004). Briefly, mice were individually habituated in an open field box (40 × 40 × 60 cm) for 15 min every day for 3 days. During the training session, each mouse was allowed to explore in the open field box with two objects for 15 min. In the 1-h and 24-h retention tests, the animals were placed in the same box for 15 min, in which one of these two objects was replaced with a novel one. Exploring preference was calculated as the ratio of the time spent in exploring one of the objects over the total time. Data were expressed as mean ± SEM and statistical significance was determined by Student's *t*-test.

Contextual fear conditioning

Mice were placed in the conditioning chamber for 3 min before the onset of the footshock. After a 2-s, 0.75 mA single footshock, the animals were allowed to stay in the chamber for another 30 s before returning to the cages. The freezing response during this 30-s period was counted as immediate freezing. After 24 h, mice were put into the same chamber for the retention test. Freezing responses were recorded for 4 min during this session. All freezing responses were sampled every 5 s and defined as complete immobility except respiration.

Microarray experiments

Male mice were decapitated rapidly and the cortex and hippocampi were dissected, pooled together and stored at −70 °C before use. The tissues were divided into three parts. Total RNA was isolated from one part of each tissue using Agilent total RNA isolation mini kit (Agilent, USA) and used for cDNA synthesis. The other two parts were used for quantitative PCR as described below. *In vitro* transcription was carried out using the Agilent low RNA input fluorescent linear amplification kit (Agilent, USA) in the presence of cy3- and cy5-CTP (PerkinElmer, USA). The fluorescent labelled cRNA was used for oligo microarray hybridization. The hybridization solution was prepared using an *in situ* hybridization kit plus (Agilent, USA). The Agilent 22K mouse oligo microarray (Agilent, USA) was used for hybridization. The hybridization reaction was carried out in the hybridization incubator for 17 h at 60 °C. The Microarray scanner system (Agilent, USA) and Feature Extraction software were used for data analysis. The log ratio values that were equal to the ratio of Cy5 processed signal to Cy3 processed signal were calculated and converted to fold changes.

Real time PCR

Quantitative PCR (qPCR) was carried out as described previously (Li *et al.*, 2005). Briefly, total RNA was extracted from the other two parts of the frozen tissues using Trizol (Invitrogen, USA). These two RNA samples and the RNA that was left from the microarray experiments were used to generate cDNA using M-MLV Reverse Transcriptase (Invitrogen, USA). The cDNA samples were used as templates for SYBR Green qPCR. The primers were designed using PrimerExpress software and synthesized by Sangon (China) (Primer sequences are listed in Supplementary material, Table S1). Glyceraldehyde-3-phosphate dehydrogenase (GAPDH) was used as a reference gene. The experiment was performed using Opticon 2 (MJ research, USA) as described previously (Rajeevan *et al.*, 2001). Gene expression levels were calculated and described

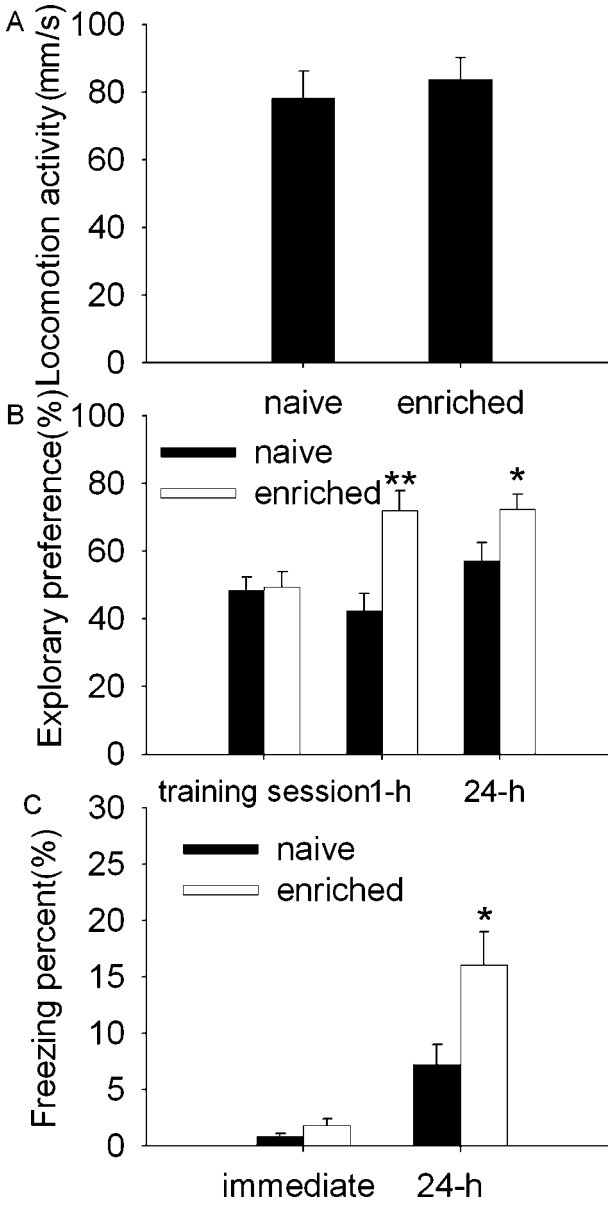

FIG. 1. Effects of EE on locomotion activity and memory performance of naive group ($n = 13$) and enriched group ($n = 15$). (A) The locomotion activity in cDKO mice after EE treatment. (B) Effects of EE on recognition memory task in cDKO mice. The enriched group showed memory improvement at 1-h and 24-h retention test. (C) Effects of EE on contextual conditioning memory in cDKO mice. Enriched group showed memory improvement 24 h after training. Data are shown as the mean ± SEM and analysed using Student's *t*-test; $*P < 0.05$, $**P < 0.01$.

as $2^{-\Delta\Delta Ct}$ values. Data were presented as mean ± SEM. Statistical significance was determined by Student's *t*-test using SigmaPlot Software (Systat Software Inc.). $P < 0.05$ was considered as statistical significance.

Histology

Seven-month-old male wild-type, naive and enriched cDKO mice, three animals per group, were used for histological analysis. Mice were deeply anaesthetized with the injection of pentobabital (50 mg/kg), and transcardially perfused with 0.9% NaCl followed by 4% paraformaldehyde. Brains were dissected, postfixed for 2 h at 4 °C, and immersed into 20% and 30% sucrose-PBS for dehydration. Coronal sections of 20 μM were cut using a cryostat (Leica, Germany). The brain sections were used for Hematoxylin-Eosin (HE) staining. Stained brain slices were examined under Leica fluorescent microscopy (Leica DM4000B, Germany). The Leica Qwin software was used to measure the thicknesses and areas of the cortex, hippocampus and ventricle of the sections. The data were expressed as mean ± SEM and analysed by Student's *t*-test.

Western blotting

Hippocampi of 7-month-old male wild-type, naive cDKO and enriched cDKO mice, five mice per group, were dissected, pooled and homogenized in cold lysis buffer (Beyotime, China) plus 1 : 100 volume of PMSF. The samples were centrifuged at 14 000 × *g* for 5 min to remove debris. The BCA kit (Beyotime, China) was used to measure the protein concentrations. Proteins were resolved by SDS-PAGE and transferred to nitrocellulose membrane (Amersham, Sweden) at 100 V for 45 min. After blocking in TBST containing 5%

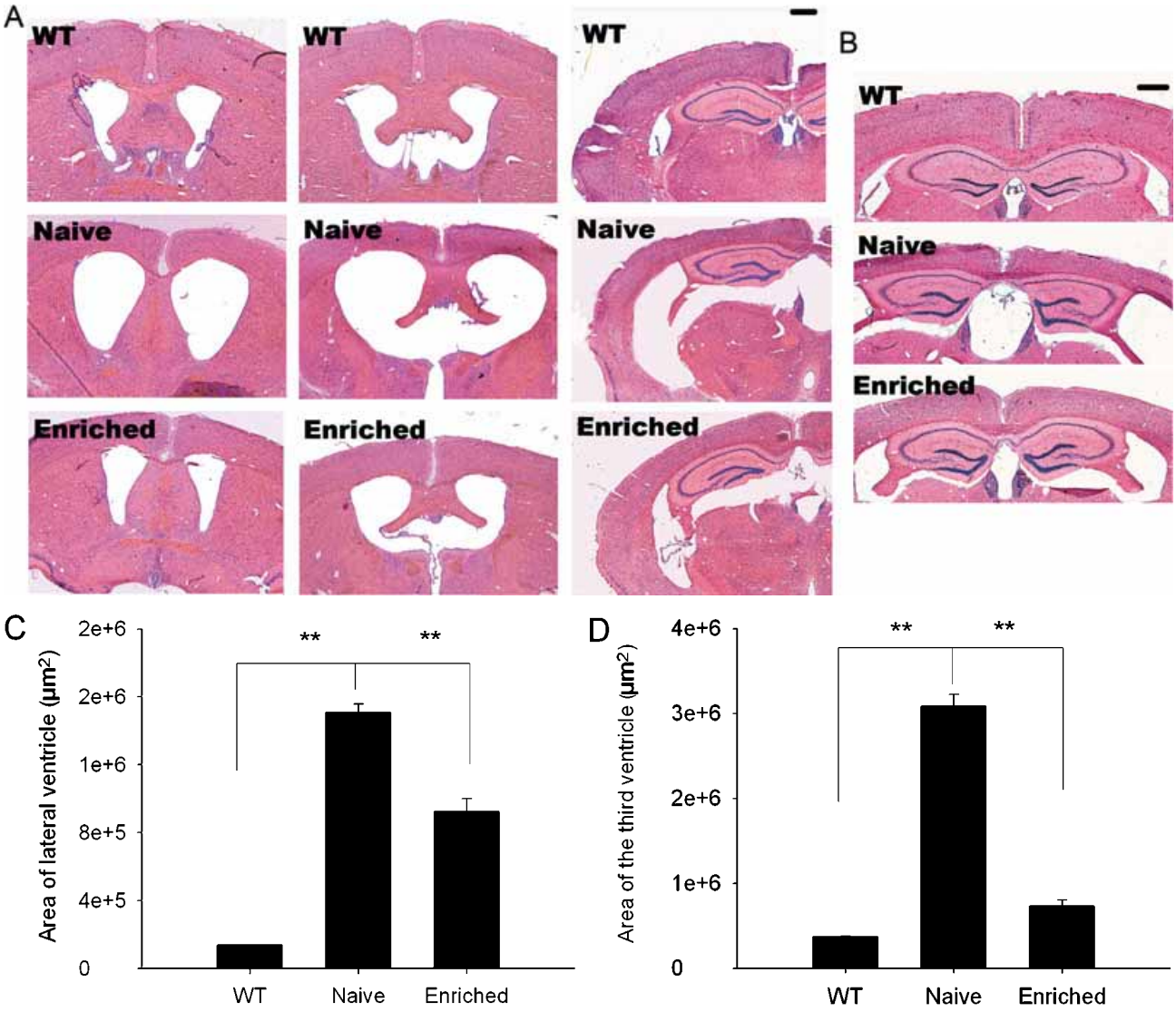

FIG. 2. Effects of EE on the enlargement of the lateral ventricles (A) and the third ventricles (B) in the brains of cDKO mice. (A) Representative lateral ventricles of different levels [frontal (Left); middle (Middle); hind (Right)]. (B) Representative third ventricles; scale bar, 500 μm. (C and D) Quantification of the areas of lateral ventricles (A) and the third ventricles (B) was performed using Qwin Lecia software. The area is expressed as the mean ± SEM (μm^2) and analysed using Student's *t*-test; $^{**}P < 0.01$; $n = 3$.

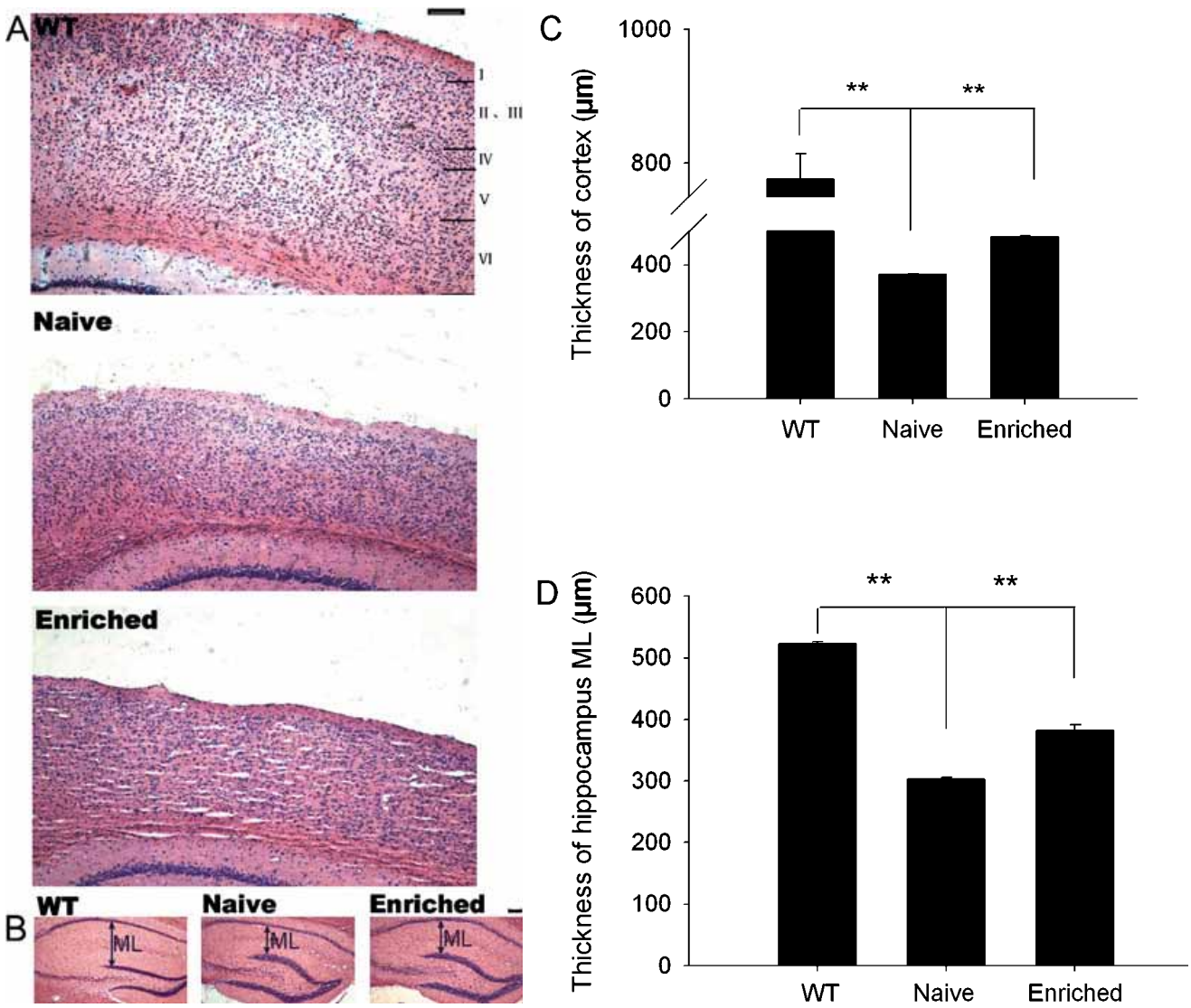

FIG. 3. Effects of EE on the forebrain degeneration in cDKO mice. (A) Representative cortex of wt (top), naive cDKO (middle) and enriched cDKO (down) mice. Scale bar, 100 μm. (B) Representative hippocampus of wt (left), naive cDKO (middle) and enriched cDKO (right) mice. The molecular layers between the CA1 pyramidal cells and dentate gyrus granule cells were indicated by the arrow (ML). Scale bar, 500 μm. (C and D) The quantification of the thickness of cortex and hippocampus ML was performed using Qwin Lecia software. The thickness was expressed as the mean ± SEM (μm) and analysed using Student's *t*-test; $^{**}P < 0.01$; $n = 3$.

TABLE 1. The differential expressions of genes associated with immunity and inflammatory response in the cortex and hippocampus of 3-month-old cDKO mice

Accession number	Gene name	Fold change
Cortex		
NM_009777	Complement component 1, q subcomponent, beta polypeptide (C1qb)	2.07
NM_009983	Cathepsin D (Ctsd)	2.09
U47328	MHC class I heavy chain precursor (H-2K(b))	2.14
NM_010745	Lymphocyte antigen 86 (Ly86)	2.22
NM_009780	Complement component 4 (within H-2S) (C4)	2.29
NM_019909	MHC (A.CA/J(H-2K-f) class I antigen (LOC56628)	2.32
NM_021281	Cathepsin S (Ctss)	2.38
NM_013706	CD52 antigen (Cd52)	2.65
NM_007572	Complement component 1, q subcomponent, alpha polypeptide (C1qa)	3.02
NM_009139	Small inducible cytokine A6 (Scya6)	11.19
Hippocampus		
NM_011336	Small inducible cytokine A27 (Scya27)	2.07
NM_021281	Cathepsin S (Ctss)	2.51
NM_009139	Small inducible cytokine A6 (Scya6)	3.86

skimmed milk powder at room temperature for 1 h, the membranes were incubated in the same solution with antibody against glial fibrillary acidic protein (GFAP; Beijing zhongshan golden bridge, China) with a dilution of 1 : 2000 and antibody against β-tubulin (Calbiochem, USA) with a dilution of 1 : 125 at room temperature for 1 h. The membranes were rinsed three times with TBST and incubated with goat anti-rabbit or goat anti-mouse IgG with a dilution of 1 : 2000 at room temperature for 45 min. After three washes with TBST, the membranes were developed using the ECL chemiluminiscence kit. The protein levels were quantified using Quantity one software (Bio-Rad, USA) and normalized with β-tubulin.

Results

EE improved memory performance in cDKO mice

We have tested the behavioural performance of cDKO mice after EE treatment for five months. Our results showed that EE did not affect locomotion in cDKO mice (Fig. 1A; $P > 0.05$). It has been reported that 6-month-old cDKO mice showed severe memory impairment (Saura *et al*., 2004). We performed the novel object recognition experiment to test whether their memory deficits could be rescued by EE exposure. Our results demonstrated that during the training session, no preference between two objects was found among these groups. However, the enriched group spent a longer time exploring the

TABLE 2. The differential expressions of genes associated with immunity and inflammatory response in the cortex of 10-month-old cDKO mice

Accession number	Gene name	Fold change
NM_010730	Annexin A1 (Anxa1)	2.01
NM_019959	C1q and tumour necrosis factor-related protein 1 (C1qtnf1)	2.22
NM_009983	Cathepsin D (Ctsd)	2.47
NM_007801	Cathepsin H (Ctsh)	2.22
NM_021281	Cathepsin S (Ctss)	2.34
NM_022325	Cathepsin Z (Ctsz)	2.46
NM_009841	CD14 antigen (Cd14)	2.22
AK021021	CD47 antigen (Rh-related antigen, integrin-associated signal transducer) (Cd47)	2.26
X53526	CD48 antigen (Cd48)	3.21
NM_013706	CD52 antigen (Cd52)	3.75
NM_007653	Cd63 antigen (Cd63)	2.35
NM_009853	CD68 antigen (Cd68)	2.89
NM_011335	Chemokine (C-C motif) ligand 21a (leucine) (Ccl21a)	0.42
NM_011337	Chemokine (C-C motif) ligand 3 (Ccl3)	8.44
NM_013652	Chemokine (C-C motif) ligand 4 (Ccl4)	5.97
NM_009139	Chemokine (C-C motif) ligand 6 (Ccl6)	4.85
NM_009892	Chitinase 3-like 3 (Chi3l3)	2.26
NM_007781	Colony stimulating factor 2 receptor, beta 2, low-affinity (granulocyte-macrophage) (Csf2rb2)	2.45
NM_007572	Complement component 1, q subcomponent, alpha polypeptide (C1qa)	3.63
NM_009777	Complement component 1, q subcomponent, beta polypeptide (C1qb)	3.01
NM_007574	Complement component 1, q subcomponent, gamma polypeptide (C1qg)	2.31
K02782	Complement component 3 (C3)	3.22
NM_009780	Complement component 4 (within H-2S) (C4)	7.42
NM_010186	Fc receptor, IgG, high affinity I (Fcgr1)	2.10
NM_010187	Fc receptor, IgG, low affinity Iib (Fcgr2b)	3.94
M25937	Glial fibrillary acidic protein (GFAP)	4.61
NM_013532	Glycoprotein 49 B (Gp49b)	2.59
NM_017370	Haptoglobin (Hp)	3.47
NM_010379	Histocompatibility 2, class II antigen A, beta 1 (H2-Ab1)	2.29
NM_008200	Histocompatibility 2, D region locus 4 (H2-D4)	2.28
BC003476	Ia-associated invariant chain (Ii)	2.43
NM_015790	Icos ligand (Icosl)	2.40
BY426609	Immunoglobulin heavy chain (J558 family) (Igh-VJ558)	8.55
NM_019633	Immunoglobulin kappa chain variable 8 (Igk-V8)	2.01
NM_030691	Immunoglobulin superfamily, member 6 (Igsf6)	3.34
AY048685	Immunoglobulin superfamily, member 7 (Igsf7)	2.92
S80963	Interleukin 13 receptor, alpha 1 (Il13ra1)	2.15
NM_134159	Interleukin 17 receptor C (Il17rc)	3.23
BC025901	Leucocyte-associated Ig-like receptor 1 (Lair1)	2.07
NM_019391	Lymphocyte specific 1 (Lsp1)	2.15
NM_008479	Lymphocyte-activation gene 3 (Lag3)	2.32
NM_010735	Lymphotoxin A (Lta)	3.25
L20315	Macrophage expressed gene 1 (Mpeg1)	2.86
L11455	Neutrophil cytosolic factor 1 (Ncf1)	2.05
NM_008694	Neutrophilic granule protein (Ngp)	6.96
U96693	Paired-Ig-like receptor B (Pirb)	5.54
NM_009114	S100 calcium binding protein A9 (calgranulin B) (S100A9)	46.19
NM_009776	Serine (or cysteine) proteinase inhibitor, clade G, member 1 (Serping1)	2.09
NM_029612	SLAM family member 9 (Slamf9)	2.88
NM_016960	Small inducible cytokine subfamily A20 (Scya20)	2.58
NM_011905	Toll-like receptor 2 (Tlr2)	4.86
NM_028075	Tumour necrosis factor receptor superfamily, member 13c (Tnfrsf13c)	2.20
NM_011691	Vav 1 oncogene (Vav1)	2.54

novel object at the 1-h and 24-h retention test, while the naive group did not exhibit significant preference over the two objects (Fig. 1B; $P < 0.05$ or 0.01).

Six-month-old cDKO mice have severe impairment of memory in the contextual fear conditioning task (Saura *et al.*, 2004). We have examined the effects of EE on memory performance. In this task, we found that naive and enriched cDKO mice displayed similar levels of freezing immediately after training ($P > 0.05$). However, when presented with the training context following a retention delay of 24 h, the enriched group significantly increased the levels of freezing (16.07 ± 2.92%) compared to the naive group (7.25 ± 1.72%; Fig. 1C; $P < 0.05$).

EE rescued the cortex and hippocampus neurodegeneration of cDKO mice

It has been reported that 6–9-month-old cDKO mice showed progressive cortical shrinkage and ventrical enlargement (Saura *et al.*, 2004). We have examined the brain morphology of 7-month-old wild-type, naive cDKO and enriched cDKO mice. HE staining

TABLE 3. The differential expressions of genes associated with immunity and inflammatory response in the hippocampus of 10-month-old cDKO mice

Accession number	Gene name	Fold change
NM_033601	B-cell leukaemia/lymphoma 3 (Bcl3)	3.36
Y17159	B-cell linker (Blnk)	4.60
NM_009735	Beta-2 microglobulin (B2m)	2.03
NM_009983*	Cathepsin D (Ctsd)*	3.49*
NM_021281*	Cathepsin S (Ctss)*	3.20*
NM_022325*	Cathepsin Z (Ctsz)*	2.76*
NM_009841*	CD14 antigen (CD14)*	2.19*
AK021021*	CD47 antigen (CD47)*	2.37*
X53526*	CD48 antigen (CD48)*	4.37*
NM_013706*	CD52 antigen (CD52)*	6.35*
NM_007651	CD53 antigen (CD53)	2.39
NM_007653*	Cd63 antigen (CD63)*	2.62*
NM_009853*	CD68 antigen (CD68)*	4.00*
NM_013489	CD84 antigen (CD84)	2.73
NM_011335*	Chemokine (C-C motif) ligand 21a (leucine) (Ccl21a)*	0.13*
NM_011337*	Chemokine (C-C motif) ligand 3 (Ccl3)*	6.15*
NM_013652*	Chemokine (C-C motif) ligand 4 (Ccl4)*	6.99*
NM_021274	Chemokine (C-X-C motif) ligand 10 (Ccl10)	0.38
NM_007572*	Complement component 1, q subcomponent, alpha polypeptide (C1qa)*	5.44*
NM_009777*	Complement component 1, q subcomponent, beta polypeptide (C1qb)*	4.10*
NM_007574*	Complement component 1, q subcomponent, gamma polypeptide (C1qg)*	2.22*
K02782*	Complement component 3 (C3)*	3.73*
NM_009780*	Complement component 4 (within H-2S) (C4)*	6.88*
NM_009888	Complement component factor H (Cfh)	2.04
NM_010185	Fc receptor, IgE, high affinity I, gamma polypeptide (Fcer1g)	2.53
NM_010186	Fc receptor, IgG, high affinity I (Fcgr1)	2.16
NM_010188*	Fc receptor, IgG, low affinity Iib (Fcgr2b)*	3.12*
M25937*	Glial fibrillary acidic protein (GFAP)*	4.42*
NM_013532*	Glycoprotein 49 B (Gp49b)*	2.25*
NM_010379	Histocompatibility 2, class II antigen A, beta 1 (H2-Ab1)	2.97
NM_010387	Histocompatibility 2, class II, locus Mb1 (H2-DMb1)	2.47
NM_008200*	Histocompatibility 2, D region locus 4 (H2-D4)*	2.29*
NM_010394	Histocompatibility 2, Q region locus 7 (H2-Q7)	2.21
BC003476*	Ia-associated invariant chain (Ii)*	2.26*
NM_015790*	Icos ligand (Icosl)*	2.01*
BY426609*	Immunoglobulin heavy chain (J558 family)*	3.36*
M30387	Immunoglobulin lambda chain 5 (Igl-5)	0.45
NM_030691*	Immunoglobulin superfamily, member 6 (Igsf6)*	2.86*
AY048685*	Immunoglobulin superfamily, member 7 (Igsf7)*	2.69*
NM_008331	Interferon-induced protein with tetratricopeptide repeats 1 (Ifit1)	0.40
S80963*	Interleukin 13 receptor, alpha 1 (Il13ra1)*	2.13*
BC025901*	Leucocyte-associated Ig-like receptor 1 (Lair1)*	2.36*
NM_008479*	Lymphocyte-activation gene 3 (Lag3)*	2.88*
U96693*	Paired-Ig-like receptor B (Pirb)*	4.29*
NM_008987	Pentaxin related gene (Ptx3)	3.05
NM_022415	Prostaglandin E synthase (Ptges)	2.21
NM_023380	SAM domain, SH3 domain and nuclear localization signals, 1 (Samsn1)	2.07
NM_009114*	S100 calcium binding protein A9 (calgranulin B) (S100A9)*	3.57*
NM_009263	Secreted phosphoprotein 1 (Spp1)	2.71
NM_009776*	Serine (or cysteine) proteinase inhibitor, clade G, member 1 (Serping1)*	2.11*
AK010014	Similar to alpha-interferon inducible protein	0.27
BC024587	SLAM family member 8 (Slamf8)	2.11
NM_009311	Tachykinin 1 (Tac1)	0.45
NM_011905*	Toll-like receptor 2 (Tlr2)*	6.01*
NM_031253	Triggering receptor expressed on myeloid cells 2a	3.90

*Genes that were also up-regulated in the cortex of 10-month-old cDKO mice compared to wild-type mice.

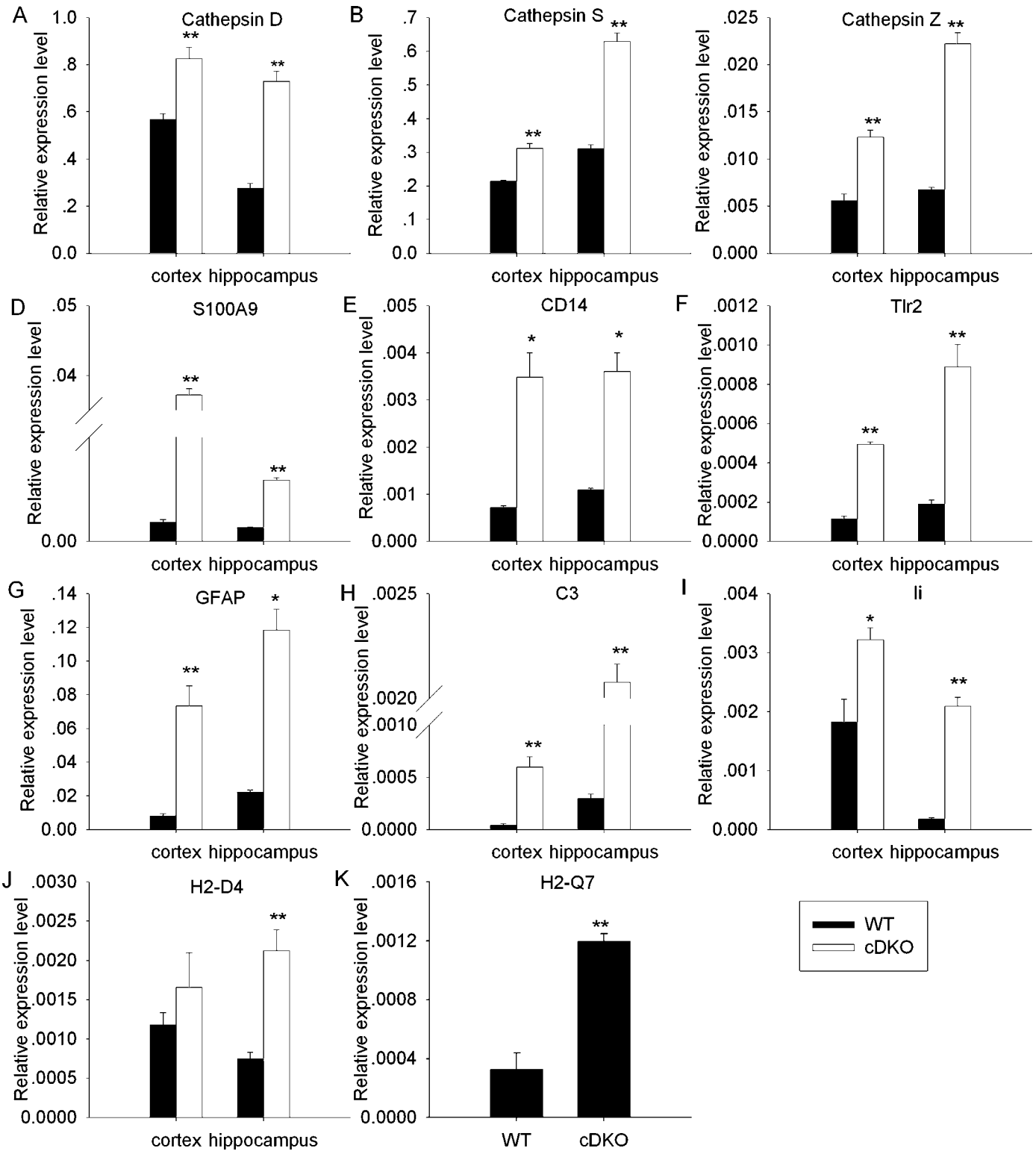

FIG. 4. Expression changes of some immunity and inflammatory-related genes in the cortex and hippocampus of 10-month-old cDKO mice. The relative mRNA levels of A (Cathepsin D), B (Cathepsin S), C (Cathepsin Z), D (S100A9), E (CD14), F (Tlr2), G (GFAP), H (C3), I (Ii) and J (H2-D4) were measured using real-time quantitative PCR in both cortex and hippocampus. K(H2-Q7) was the real PCR result of hippocampus. Relative expression levels were calculated as the ratio of the target gene expression level to the GAPDH expression level in the same sample. Data are shown as the mean ± SEM and analysed using Student's *t*-test, $*P < 0.05$, $**P < 0.01$.

was performed to examine for neurodegeneration in cDKO mice. We found that cDKO brains showed immense enlargement of the lateral ventricles in comparison with the brains of wild-type mice, while the enlargement was significantly less in the enriched mice (Fig. 2A and C). Similarly, the third ventricles were massively enlarged in the 7-month-old cDKO mice, while the enlargement was significantly

reduced in the enriched mice (Fig. 2B and D). Furthermore, we found that cortical thickness was greatly reduced and the classic six layers of the cortex were not present in the 7-month-old cDKO mice, while the cortical thickness of enriched mice was significantly increased (Fig. 3A and C). We also observed that the molecular layers between hippocampal CA1 pyramidal cells and dentate gyrus were reduced in the naive cDKO mice and the morphological changes were rescued by EE treatment (Fig. 3B and D).

Up-regulation of inflammation-related genes in the brain of 3-month-old and 10-month-old cDKO mice

Previous studies showed that young cDKO mice exhibited normal brain morphology, mild memory impairment, abnormal synaptic plasticity, NMDA receptor activity reduction and gene expression changes (Saura *et al*., 2004). However, 10-month-old cDKO mice showed severe neurodegenerative and memory impairment phenotypes (Feng *et al*., 2004). To determine the changes associated with the progressive neuropathology at the molecular level in cDKO mice, we have systematically analysed the gene expression profiles in the hippocampus and cortex of 3- and 10-month-old wild-type and cDKO mice using oligonucleotide microarray technology. A total of 22 000 genes and expressed sequence tags were examined in tissues from five 3-month-old wild-type and five 3-month-old cDKO mice. The results showed that the expression levels of 56 and 46 genes were altered more than two-fold in the cortex and hippocampus of cDKO mice, respectively (supplementary Tables S2 and S3). Notably, ten genes involved in immunity and inflammatory response in the cortex and three in the hippocampus were up-regulated in cDKO mice (Table 1). Next, we examined the gene expression profiles of 10-month-old cDKO mice using three mice per group. The results demonstrated that 355 and 281 genes changed their expression levels in the cortex and hippocampus, respectively (supplementary Tables S4 and S5). Interestingly, a large number of these genes were up-regulated (263 genes in the cortex and 217 in the hippocampus). Based on their physiological functions, the differently expressed genes could be classified into multiple signal pathways, including immunity and inflammatory responses, metabolism, transcription, transport, structure, and cell adhesion. We also observed that many immunity and inflammation-related genes were differentially regulated in both the cortex and hippocampus of cDKO mice (Tables 2 and 3). It is worth noting that most of these genes, 52 of 53 genes in the cortex and 50 of 56 genes in the hippocampus, increased their expression levels. These up-regulated genes include Cathepsins, CD antigens, chemokine ligands, complement components, Fc receptors, and histocompatibility-related proteins. Importantly, 33 genes were commonly regulated in both cortex and hippocampus of the cDKO mice, including the markers for astrocyte and microglia.

Eleven up-regulated immunity and inflammation-related genes were selected for real-time PCR analysis to validate the microarray data. We used pooled tissues for the real-time PCR analysis. The results

TABLE 4. The differential expressions of genes associated with immunity and inflammatory response in the hippocampus of enriched mice

Accession number	Gene name	Fold change
NM_008620	Macrophage activation 2 (Mpa2)	0.38
NM_009735*	Beta-2 microglobulin (B2m)*	0.45*
K02782*	Complement component 3 (C3)*	0.44*
NM_011333	Chemokine (C-C motif) ligand 2 (Ccl2)	0.20
NM_013653	Chemokine (C-C motif) ligand 5 (Ccl5)	0.20
NM_021443	Chemokine (C-C motif) ligand 8 (Ccl8)	0.47
NM_021274	Chemokine (C-X-C motif) ligand 10 (Ccl10)	0.05
NM_015783	Interferon, alpha-inducible protein (G1p2)	0.23
NM_010260	Guanylate nucleotide binding protein 2 (Gbp2)	0.36
NM_018734	Guanylate nucleotide binding protein 3 (Gbp3)	0.34
NM_008198	Histocompatibility 2, complement component factor B (H2-bf)	0.29
NM_008200*	Histocompatibility 2, D region locus 4 (H2-D4)*	0.45*
U47328	Histocompatibility 2, K1, K region (H2-K1)	0.40
NM_010393	Histocompatibility 2, D region locus 1 (H2-D1)	0.48
NM_019909	Histocompatibility 2, Q region locus 1 (H2-Q1)	0.39
NM_010394*	Histocompatibility 2, Q region locus 7 (H2-Q7)*	0.42*
NM_010398	Histocompatibility 2, T region locus 23 (H2-T23)	0.47
NM_008326	Interferon inducible protein 1 (Ifi1)	0.41
NM_008329	Interferon, gamma-inducible protein 16 (Ifi16)	0.38
NM_008327	Interferon activated gene 202B (Ifi202b)	0.24
AK010014	Interferon, alpha-inducible protein 27 (Ifi27)	0.12
NM_008331	Interferon-induced protein with tetratricopeptide repeats 1 (Ifit1)	0.17
NM_008332	Interferon-induced protein with tetratricopeptide repeats 2 (Ifit2)	0.50
NM_010501	Interferon-induced protein with tetratricopeptide repeats 3 (Ifit3)	0.33
BY426609*	Immunoglobulin heavy chain (J558 family) (Igh-VJ558)*	0.28*
BC003476*	Ia-associated invariant chain (Ii)*	0.50*
NM_013606	Myxovirus (influenza virus) resistance 2 (Mx2)	0.36
AK037025	2′-5′ oligoadenylate synthetase 1F (Oas1f)	0.46
AB067535	2′-5′ oligoadenylate synthetase 2 (Oas2)	0.40
NM_011854	2′-5′ oligoadenylate synthetase-like 2 (Oasl2)	0.31
NM_021893	Programmed cell death 1 ligand 1 (Pdcd1lg1)	0.30
U96693*	Paired-Ig-like receptor B (Pirb)*	0.43*
NM_010724	Proteosome (prosome, macropain) subunit, beta type 8 (Psmb8)	0.43
NM_009114*	S100 calcium binding protein A9 (calgranulin B) (S100A9)*	0.31*
NM_009396	Tumour necrosis factor, alpha-induced protein 2 (Tnfaip2)	0.41

*Genes that were up-regulated in the hippocampus of 10-month-old cDKO mice compared to wild-type mice.

confirmed that all of the above mentioned genes increased their expression levels in the cortex and hippocampus of 10-month-old cDKO mice (Fig. 4). Lysosomal proteases Cathepsin D, S and Z were up-regulated by more than two-fold (Fig. 4A–C; $P < 0.01$). An inflammatory marker, S100 calcium binding protein A9 (S100A9), was increased by 46.2-fold in the cortex and 4.4-fold in the hippocampus (Fig. 4D; $P < 0.01$). The astrocyte marker, GFAP, was up-regulated by 4.6-fold in the cortex and 5.3-fold in the hippocampus (Fig. 4G; $P < 0.01$ or $P < 0.05$). Other genes involved in immunity or inflammatory responses, such as CD14 antigen (CD14), toll-like receptor 2 (Tlr2), complement component 3 (C3), Ia-associated invariant chain (Ii), histocompatibility 2, D region locus 4 (H2–D4) and histocompatibility 2, Q region locus 7 (H2–Q7), showed induction of expression (Fig. 4E, F and H–K; $P < 0.05$ or $P < 0.01$) in the hippocampus, while CD14, Tlr2, C3 and Ii were up-regulated in the cortex of 10-month-old cDKO mice (Fig. 4E, F, H and I; $P < 0.05$ or $P < 0.01$).

EE reduced the expression of inflammation-related genes in hippocampus

We conducted microarray and real-time quantitative PCR experiments to elucidate the molecular basis underlying the EE alleviated neuropathology. First, we performed oligonucleotide microarray analysis using RNA from the hippocampi of five 7-month-old naive and five enriched cDKO mice. We found that the expression levels of 90 genes were altered after EE treatment (supplementary Table S6). Thirty-four genes involved in immunity and inflammatory responses were down-regulated in the hippocampus of enriched group (Table 4). Notably, some up-regulated genes in the hippocampus of cDKO mice, such as B2m, C3, H2–D4, H2–Q7, Ii, Igh-VJ558, Pirb and S100A9, were down-regulated after EE treatment (Table 3). Next, we performed real-time PCR experiments with pooled samples to confirm the microarray data. The expression level of complement component C3 was reduced in the enriched mice (Fig. 5A; $P < 0.01$). A number of immunity-associated genes, such as Ii, H2–D4 and H2–Q7, were down-regulated after EE treatment (Fig. 5B–D; $P < 0.01$ or 0.05). The inflammatory marker gene, S100A9, was decreased by 2.5-fold in the hippocampus of enriched mice (Fig. 5E; $P < 0.01$). Furthermore, we measured the effects of EE on the expression of Cathepsin D, Cathepsin S and CD14 genes that had been found to be up-regulated in the hippocampus of cDKO mice. Cathepsin S was significantly down-regulated after EE (Fig. 5G; $P < 0.01$). The expression of inflammatory gene CD14 was decreased by 2.8-fold in the hippocampus of enriched group (Fig. 5H; $P < 0.01$).

Astrocytes have been shown to be associated with immunity and inflammatory response in the brain. The expression level of the astrocyte marker, GFAP, was up-regulated in the brain of cDKO mice. We examined the effects of EE on mRNA and protein levels of GFAP using quantitative PCR and Western blot techniques. The results demonstrated that GFAP mRNA was down-regulated in cDKO

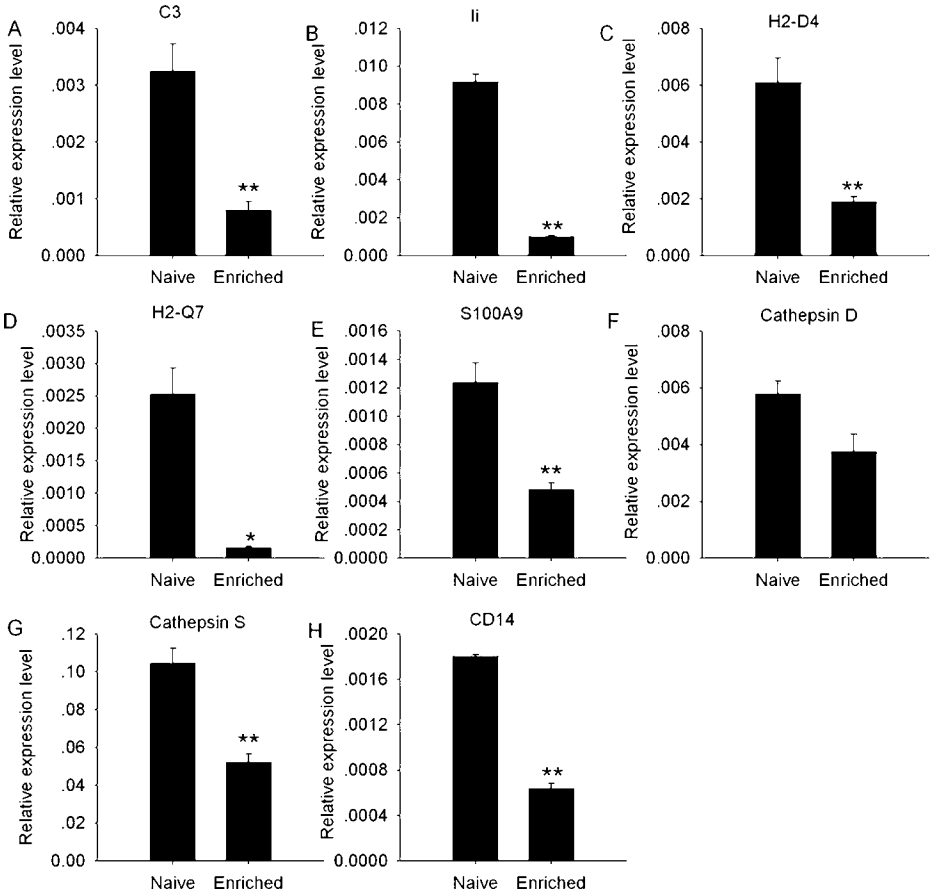

FIG. 5. Effects of EE on the expression of some immunity and inflammatory-related genes in the hippocampus of 7-month-old cDKO mice. The relative mRNA levels of A (C3), B (Ii), C (H2-D4), D (H2-Q7), E (S100A9), F (Cathepsin D), G (Cathepsin S) and H (CD14) were measured using real-time quantitative PCR and calculated as the ratio of the target gene expression level to GAPDH expression level in the same sample. Data are shown as the mean ± SEM and analysed using Student's *t*-test, $*P < 0.05$, $**P < 0.01$.

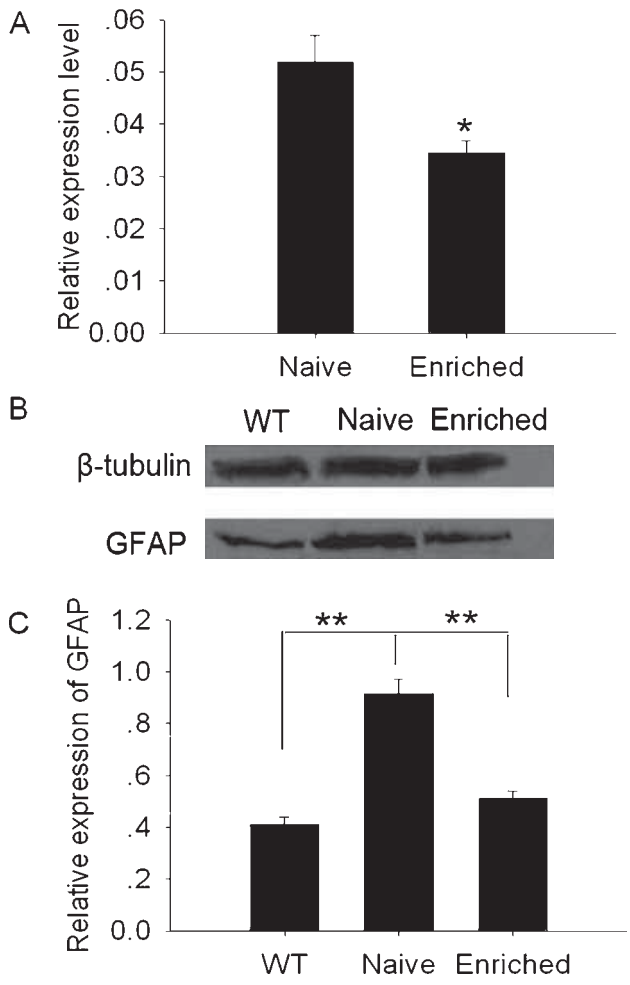

FIG. 6. Effects of EE on mRNA and protein expression of GFAP in hippocampus of cDKO mice. (A) Real-time PCR results showed that relative mRNA levels of GFAP to GAPDH were significantly down-regulated by EE. Data are shown as the mean ± SEM, Student's *t*-test; $*P < 0.05$. (B) Western blotting analysis for GFAP ($n = 5$). β-tubulin was used as a loading control. (C) Quantification of protein level of GFAP was performed using Quantity one software (Bio-rad) and normalized with β-tubulin. Data are shown as the mean ± SEM and analysed using Student's *t*-test; $**P < 0.01$.

hippocampus after EE exposure (Fig. 6A; $P < 0.05$). Moreover, the immunoblotting analysis showed that the GFAP protein was increased in the hippocampus of cDKO mice, while it was reduced after EE treatment (Fig. 6B and C).

Discussion

It has been shown that inactivation of PS genes in the adult forebrain of mice resulted in progressive impairment of learning and memory, astrogliosis, tau protein hyperphosphorylation (Saura *et al*., 2004) and forebrain degeneration (Feng *et al*., 2004). These phenotypes of the cDKO mice are similar to the neuropathology of AD, indicating that double knockout mice could be a useful animal model for AD. However, unlike AD patients, cDKO mice showed a reduction in the level of Aβ (Beglopoulos *et al*., 2004). In this report, we have investigated the underlying cellular and molecular events and assessed the effects of 5-months EE treatment on the neurodegenerative phenotypes. We found that the exposure of cDKO mice to an enriched environment for 5 months resulted in an improvement of memory performance and a reduction of both forebrain degeneration and astrogliosis in the hippocampus.

EE is a well-established approach that has significant benefits on both wild-type and brain disease animal models, including Alzheimer's disease, Parkinson's disease, Huntington's disease, fragile and Down syndrome, and various forms of brain injury (Li & Tang, 2005; Nithianantharajah & Hannan, 2006). A number of groups have examined the effects of EE on amyloid deposition and cognitive function in AD animal models, such as APPsw transgenic mice and mice coexpressing familial AD-linked APP and PS1 variants (APPswe × PS1ΔE9) (Jankowsky *et al*., 2003; Arendash *et al*., 2004; Lazarov *et al*., 2005). Their results have shown that EE altered the Aβ deposition and mitigated the cognitive deficits in the AD animal models (Arendash *et al*., 2004; Jankowsky *et al*., 2005). In another AD animal model expressing both human APP (V717F) and PS1 (M146L) mutants, EE was able to protect the animal against cognitive impairment through both amyloid dependent and independent mechanisms (Costa *et al*., 2007). More recently, it has been shown that EE can possibly restore learning ability and access to long-term memory in memory-impaired CK-p25 transgenic mice. There is extensive evidence that the effect of EE is associated with chromatin modification by increasing histone-tail acetylation (Fischer *et al*., 2007).

DNA microarray technology is a useful tool to dissect the mechanism underlying brain dysfunction and ageing (Wu & Hu, 2006). To understand the molecular basis of neurodegenerative phenotypes, we have analysed the gene expression profiles in the brains of 3- and 10-month-old cDKO mice. Our results have revealed that 56 and 46 genes changed their expression levels in the cortex and hippocampus of 3-month-old cDKO mice, while 355 and 281 genes changed their expression levels in the cortex and hippocampus of 10-month-old cDKO mice, respectively. Previous studies also revealed that a number of inflammation-related genes were up-regulated in the cortex of 6-month-old cDKO mice (Beglopoulos *et al*., 2004). These results strongly suggest that immunologic and inflammatory responses could play an important role in the neuropathology of AD. It has been shown that the expression of cathepsin S, a lysosomal protease important for normal histocompatibility class II-dependent immunity (Shi *et al*., 1999), was induced in the brain of AD patient (Lemere *et al*., 1995). The complement system has also been found to be involved in the inflammatory responses in AD brains (Tenner, 2001). Indeed, C1q mRNA level was increased by 10–80-fold in AD-affected brain regions. In addition, S100A9, an inflammatory marker, was significantly elevated in the brains of AD patients (Shepherd *et al*., 2006). Taken together, these results indicate that the induction of inflammatory responses is associated with AD neurodegeneration.

It is interesting to note that a number of inflammation-related genes that have been shown to be up-regulated in 10-month-old cDKO mice are down-regulated in the hippocampus of enriched mice. Furthermore, we found that the level of GFAP protein, a marker of the main immunity cell, the astrocyte, was strongly elevated in the hippocampus of 7-month-old cDKO mice and the elevation was significantly inhibited after EE treatment. These results suggest that the beneficial effects of EE on the cDKO mice might be related to the inhibition of the up-regulation of immunity and inflammation-associated genes in the hippocampus.

In summary, a significant activation of inflammatory response was observed in the cortex and hippocampus of cDKO mice. The up-regulation of a number of inflammation-related genes was reversed after EE treatment. This effect of EE may partially explain the molecular mechanisms underlying the improvement of the memory performance and the reduction of forebrain degeneration.

Supplementary material

The following supplementary material may be found on www.blackwell-synergy.com

Table S1. Primers used in the real time PCR experiments.

Table S2. The differentiated expressed genes in the cerebral cortex of 3-month-old PS cDKO mice.

Table S3. The differentiated expressed genes in the hippocampus of 3-month-old PS cDKO mice.

Table S4. The differentiated expressed genes in the cerebral cortex of 10-month-old PS cDKO mice.

Table S5. The differentiated expressed genes in the hippocampus of 10-month-old PS cDKO mice.

Table S6. Enrichment-induced gene expression profile change in the hippocampus of cDKO mice.

Acknowledgements

This work was supported by the grants from Ministry of Science and Technology of China (973 project 2003CB716601), Shanghai Commission for Science and Technology (06DZ19003), and Shanghai Commission for Education. We thank Dr Herbert Meltzer for critical reading and editing the manuscript.

Abbreviations

Aβ, β-amyloid; AD, Alzheimer's disease; C3, complement component 3; CD14, CD14 antigen; cDKO, conditional double knock out; EE, environmental enrichment; GAPDH, glyceraldehyde-3-phosphate dehydrogenase; GFAP, glial fibrillary acidic protein; H2–D4, histocompatibility 2, D region locus 4; H2–Q7, histocompatibility 2, Q region locus 7; Ii, Ia-associated invariant chain; PS, presenilin; S100A9, S100 calcium binding protein A9; Tlr2, toll-like receptor 2.

Reference

Arendash, G.W., Garcia, M.F., Costa, D.A., Cracchiolo, J.R., Wefes, I.M. & Potter, H. (2004) Environmental enrichment improves cognition in aged Alzheimer's transgenic mice despite stable beta-amyloid deposition. *Neuroreport*, **15**, 1751–1754.

Beglopoulos, V., Sun, X., Saura, C.A., Lemere, C.A., Kim, R.D. & Shen, J. (2004) Reduced beta-amyloid production and increased inflammatory responses in presenilin conditional knock-out mice. *J. Biol. Chem.*, **279**, 46907–46914.

Costa, D.A., Cracchiolo, J.R., Bachstetter, A.D., Hughes, T.F., Bales, K.R., Paul, S.M., Mervis, R.F., Arendash, G.W. & Potter, H. (2007) Enrichment improves cognition in AD mice by amyloid-related and unrelated mechanisms. *Neurobiol. Aging*, **28**, 831–844.

De Strooper, B., Saftig, P., Craessaerts, K., Vanderstichele, H., Guhde, G., Annaert, W., Von Figura, K. & Van Leuven, F. (1998) Deficiency of presenilin-1 inhibits the normal cleavage of amyloid precursor protein. *Nature*, **391**, 387–390.

van Dellen, A., Blakemore, C., Deacon, R., York, D. & Hannan, A.J. (2000) Delaying the onset of Huntington's in mice. *Nature*, **404**, 721–722.

Diamond, M.C., Law, F., Rhodes, H., Lindner, B., Rosenzweig, M.R., Krech, D. & Bennett, E.L. (1966) Increases in cortical depth and glia numbers in rats subjected to enriched environment. *J. Comp. Neurol.*, **128**, 117–126.

Donoviel, D.B., Hadjantonakis, A.K., Ikeda, M., Zheng, H., Hyslop, P.S. & Bernstein, A. (1999) Mice lacking both presenilin genes exhibit early embryonic patterning defects. *Genes Dev.*, **13**, 2801–2810.

Duffy, S.N., Craddock, K.J., Abel, T. & Nguyen, P.V. (2001) Environmental enrichment modifies the PKA-dependence of hippocampal LTP and improves hippocampus-dependent memory. *Learn. Mem.*, **8**, 26–34.

Faherty, C.J., Raviie Shepherd, K., Herasimtschuk, A. & Smeyne, R.J. (2005) Environmental enrichment in adulthood eliminates neuronal death in experimental Parkinsonism. *Brain Res. Mol. Brain Res.*, **134**, 170–179.

Feng, R., Rampon, C., Tang, Y.P., Shrom, D., Jin, J., Kyin, M., Sopher, B., Miller, M.W., Ware, C.B., Martin, G.M., Kim, S.H., Langdon, R.B., Sisodia, S.S. & Tsien, J.Z. (2001) Deficient neurogenesis in forebrain-specific presenilin-1 knockout mice is associated with reduced clearance of hippocampal memory traces. *Neuron*, **32**, 911–926.

Feng, R., Wang, H., Wang, J., Shrom, D., Zeng, X. & Tsien, J.Z. (2004) Forebrain degeneration and ventricle enlargement caused by double knockout of Alzheimer's presenilin-1 and presenilin-2. *Proc. Natl Acad. Sci. USA*, **101**, 8162–8167.

Fischer, A., Sananbenesi, F., Wang, X., Dobbin, M. & Tsai, L.H. (2007) Recovery of learning and memory is associated with chromatin remodelling. *Nature*, **447**, 178–182.

Frick, K.M. & Fernandez, S.M. (2003) Enrichment enhances spatial memory and increases synaptophysin levels in aged female mice. *Neurobiol. Aging*, **24**, 615–626.

Haass, C. (1997) Presenilins: genes for life and death. *Neuron*, **18**, 687–690.

Hockly, E., Cordery, P.M., Woodman, B., Mahal, A., van Dellen, A., Blakemore, C., Lewis, C.M., Hannan, A.J. & Bates, G.P. (2002) Environmental enrichment slows disease progression in R6/2 Huntington's disease mice. *Ann. Neurol.*, **51**, 235–242.

Jankowsky, J.L., Melnikova, T., Fadale, D.J., Xu, G.M., Slunt, H.H., Gonzales, V., Younkin, L.H., Younkin, S.G., Borchelt, D.R. & Savonenko, A.V. (2005) Environmental enrichment mitigates cognitive deficits in a mouse model of Alzheimer's disease. *J. Neurosci.*, **25**, 5217–5224.

Jankowsky, J.L., Xu, G., Fromholt, D., Gonzales, V. & Borchelt, D.R. (2003) Environmental enrichment exacerbates amyloid plaque formation in a transgenic mouse model of Alzheimer disease. *J. Neuropathol. Exp. Neurol.*, **62**, 1220–1227.

de Jong, I.C., Prelle, I.T., van de Burgwal, J.A., Lambooij, E., Korte, S.M., Blokhuis, H.J. & Koolhaas, J.M. (2000) Effects of environmental enrichment on behavioral responses to novelty, learning, and memory, and the circadian rhythm in cortisol in growing pigs. *Physiol. Behav.*, **68**, 571–578.

Kempermann, G., Kuhn, H.G. & Gage, F.H. (1997) More hippocampal neurons in adult mice living in an enriched environment. *Nature*, **386**, 493–495.

Klintsova, A.Y. & Greenough, W.T. (1999) Synaptic plasticity in cortical systems. *Curr. Opin. Neurobiol.*, **9**, 203–208.

Kolb, B. & Gibb, R. (1991) Environmental enrichment and cortical injury: behavioral and anatomical consequences of frontal cortex lesions. *Cereb. Cortex*, **1**, 189–198.

Lazarov, O., Robinson, J., Tang, Y.P., Hairston, I.S., Korade-Mirnics, Z., Lee, V.M., Hersh, L.B., Sapolsky, R.M., Mirnics, K. & Sisodia, S.S. (2005) Environmental enrichment reduces Abeta levels and amyloid deposition in transgenic mice. *Cell*, **120**, 701–713.

Lemere, C.A., Munger, J.S., Shi, G.P., Natkin, L., Haass, C., Chapman, H.A. & Selkoe, D.J. (1995) The lysosomal cysteine protease, cathepsin S, is increased in Alzheimer's disease and Down syndrome brain. An immunocytochemical study. *Am. J. Pathol.*, **146**, 848–860.

Lessard, N., Lepore, F., Poirier, P., Villemagne, J. & Lassonde, M. (1999) Localization of moving sounds by hemispherectomized subjects. *Behav. Brain Res.*, **104**, 37–49.

Levy-Lahad, E., Wasco, W., Poorkaj, P., Romano, D.M., Oshima, J., Pettingell, W.H., Yu, C.E., Jondro, P.D., Schmidt, S.D., Wang, K., Crowley, A.C., Fu, Y.H., Guenette, S.Y., Galas, D., Nemens, E., Wijsman, E.M., Bird, T.D., Schellenberg, G.D. & Tanzi, R.E. (1995) Candidate gene for the chromosome 1 familial Alzheimer's disease locus. *Science*, **269**, 973–977.

Li, L. & Tang, B.L. (2005) Environmental enrichment and neurodegenerative diseases. *Biochem. Biophys. Res. Commun.*, **334**, 293–297.

Li, X., Yang, Q. & Hu, Y. (2005) Gene expression profiling reveals the mechanism of action of anticonvulsant drug QYS. *Brain Res. Bull.*, **66**, 99–105.

Need, A.C., Irvine, E.E. & Giese, K.P. (2003) Learning and memory impairments in Kv beta 1.1-null mutants are rescued by environmental enrichment or ageing. *Eur. J. Neurosci.*, **18**, 1640–1644.

Nilsson, M., Perfilieva, E., Johansson, U., Orwar, O. & Eriksson, P.S. (1999) Enriched environment increases neurogenesis in the adult rat dentate gyrus and improves spatial memory. *J. Neurobiol.*, **39**, 569–578.

Nithianantharajah, J. & Hannan, A.J. (2006) Enriched environments, experience-dependent plasticity and disorders of the nervous system. *Nature Rev. Neurosci.*, **7**, 697–709.

Price, D.L. & Sisodia, S.S. (1998) Mutant genes in familial Alzheimer's disease and transgenic models. *Annu. Rev. Neurosci.*, **21**, 479–505.

Rajeevan, M.S., Ranamukhaarachchi, D.G., Vernon, S.D. & Unger, E.R. (2001) Use of real-time quantitative PCR to validate the results of cDNA array and differential display PCR technologies. *Methods*, **25**, 443–451.

Rampon, C., Tang, Y.P., Goodhouse, J., Shimizu, E., Kyin, M. & Tsien, J.Z. (2000) Enrichment induces structural changes and recovery from nonspatial memory deficits in CA1 NMDAR1-knockout mice. *Nature Neurosci.*, **3**, 238–244.

Rosenzweig, M.R. & Bennett, E.L. (1969) Effects of differential environments on brain weights and enzyme activities in gerbils, rats, and mice. *Dev. Psychobiol.*, **2**, 87–95.

Saura, C.A., Choi, S.Y., Beglopoulos, V., Malkani, S., Zhang, D., Shankaranarayana Rao, B.S., Chattarji, S., Kelleher, R.J., 3rd, Kandel, E.R., Duff, K., Kirkwood, A. & Shen, J. (2004) Loss of presenilin function causes impairments of memory and synaptic plasticity followed by age-dependent neurodegeneration. *Neuron*, **42**, 23–36.

Shepherd, C.E., Goyette, J., Utter, V., Rahimi, F., Yang, Z., Geczy, C.L. & Halliday, G.M. (2006) Inflammatory S100A9 and S100A12 proteins in Alzheimer's disease. *Neurobiol Aging*, **27**, 1554–1563.

Shi, G.P., Villadangos, J.A., Dranoff, G., Small, C., Gu, L., Haley, K.J., Riese, R., Ploegh, H.L. & Chapman, H.A. (1999) Cathepsin S required for normal MHC class II peptide loading and germinal center development. *Immunity*, **10**, 197–206.

Tenner, A.J. (2001) Complement in Alzheimer's disease: opportunities for modulating protective and pathogenic events. *Neurobiol. Aging*, **22**, 849–861.

Williams, B.M., Luo, Y., Ward, C., Redd, K., Gibson, R., Kuczaj, S.A. & McCoy, J.G. (2001) Environmental enrichment: effects on spatial memory and hippocampal CREB immunoreactivity. *Physiol. Behav.*, **73**, 649–658.

Winocur, G. (1998) Environmental influences on cognitive decline in aged rats. *Neurobiol. Aging*, **19**, 589–597.

Woodcock, E.A. & Richardson, R. (2000) Effects of environmental enrichment on rate of contextual processing and discriminative ability in adult rats. *Neurobiol. Learn. Mem.*, **73**, 1–10.

Wu, P. & Hu, Y.H. (2006) Definition of genes and paths involved in Alzheimer's disease: Using gene expression profiles and chemical genetics at the mouse brain level. *Curr. Genom.*, **7**, 293–300.

Zhu, J., Apparsundaram, S., Bardo, M.T. & Dwoskin, L.P. (2005) Environmental enrichment decreases cell surface expression of the dopamine transporter in rat medial prefrontal cortex. *J. Neurochem.*, **93**, 1434–1443.